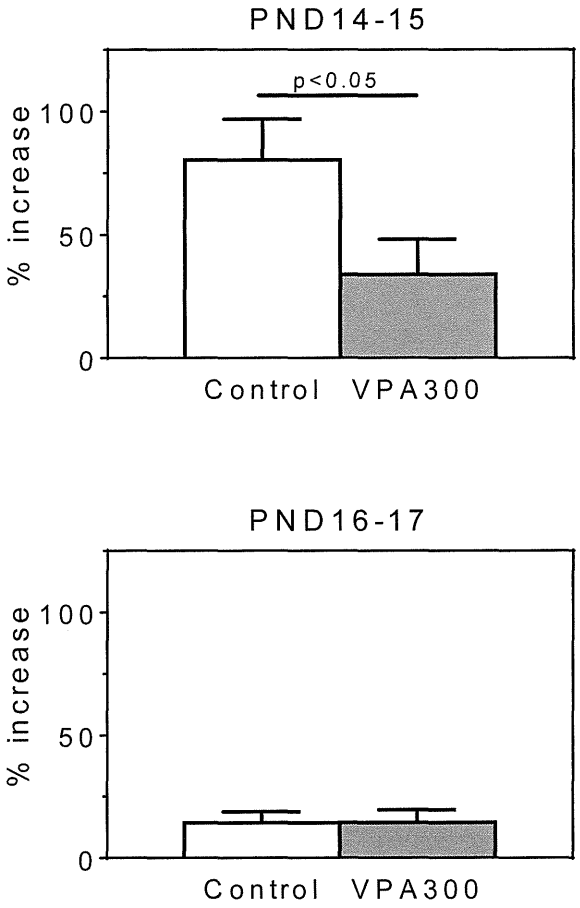

図 7. 集合スパイク電位（PS）振幅に対する $GABA_A$受容体拮抗薬ビククリンの増強作用

開眼前期（PND14-15）および開眼期（PND16-17）における集合スパイク電位（PS）振幅（刺激電流値 600 μ A）に対する $GABA_A$受容体拮抗薬ビククリン（BMI）の増強作用とこれに対する VPA 胎生期曝露の影響。変化率（%increase）は次式で求められている。

%increase＝(BMI 存在下の応答/非存在下の応答 - 1)×100

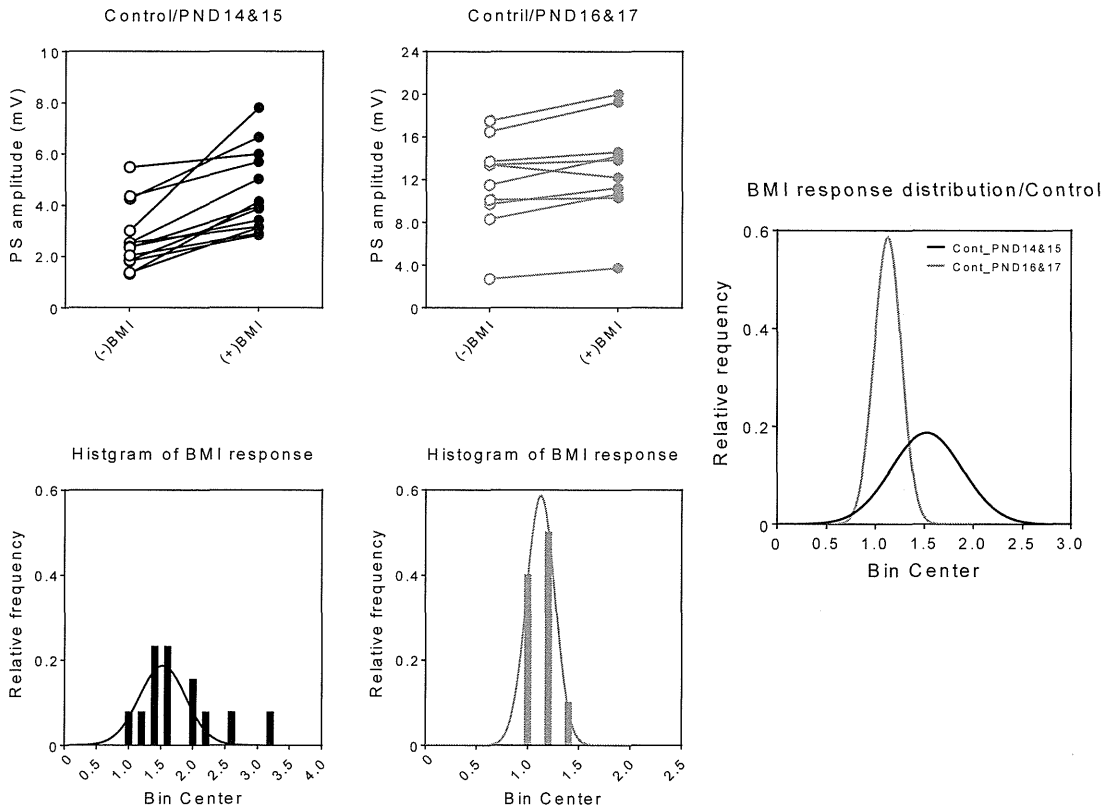

図 8. 開眼前期（PND14-15）および開眼期（PND16-17）における VPA 対照群から得られた $GABA_A$受容体拮抗薬ビククリン（BMI）存在下、非存在下での集合スパイク電位（PS）振幅（刺激電流値 600 μ A）、および BMI による増強率の分布近似曲線。

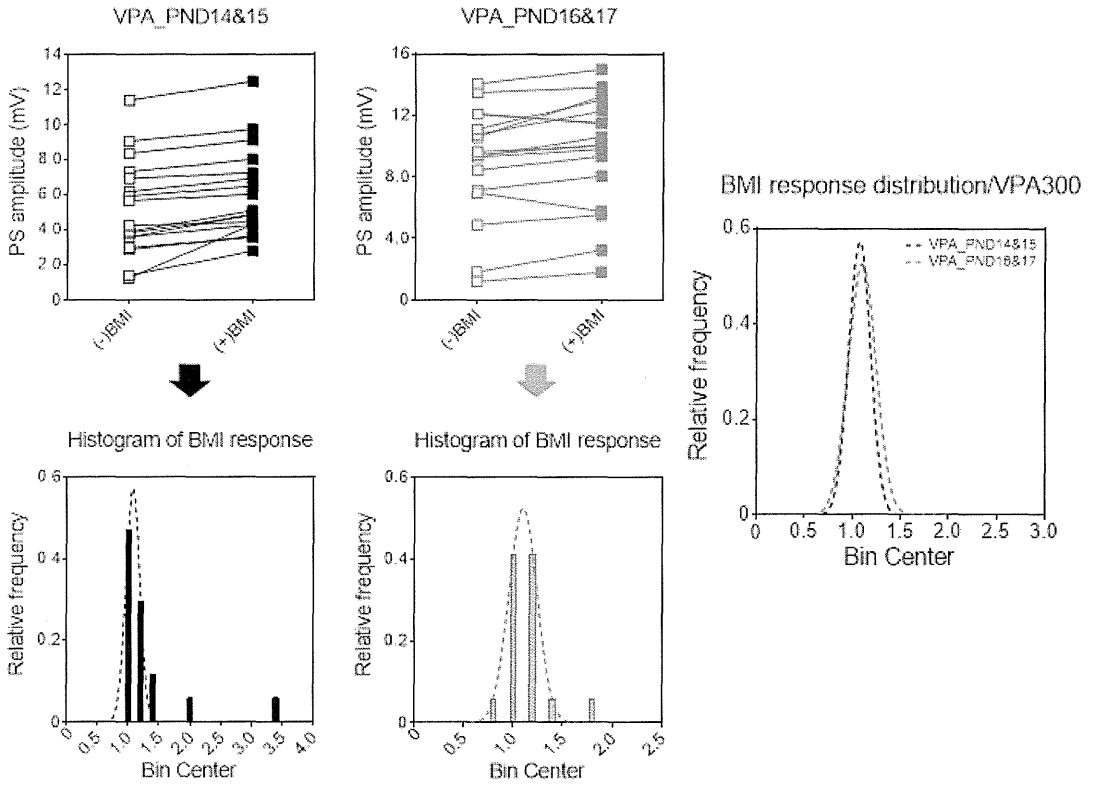

図 9. 開眼前期（PND14-15）および開眼期（PND16-17）における VPA300 群から得られた $GABA_A$受容体拮抗薬ビククリン（BMI）存在下、非存在下での集合スパイク電位（PS）振幅（刺激電流値 600 μ A）、および BMI による増強率の分布近似曲線

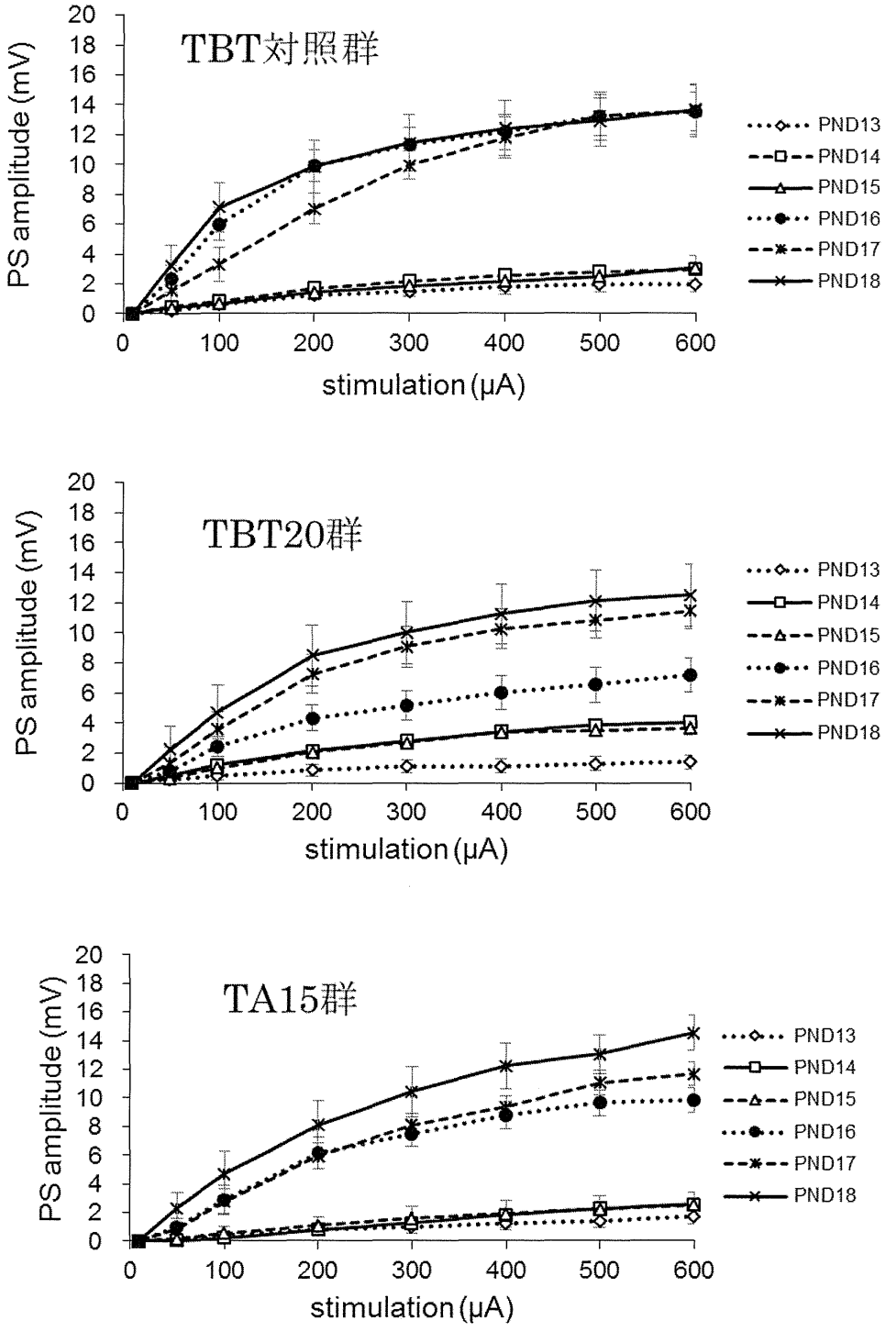

図 10. TBT（20 mg/kg）、TA（15 mg/kg）を胎生期に曝露された仔ラットを用いて、生後日齢毎に得られた集合スパイク電位（PS）の刺激応答性。

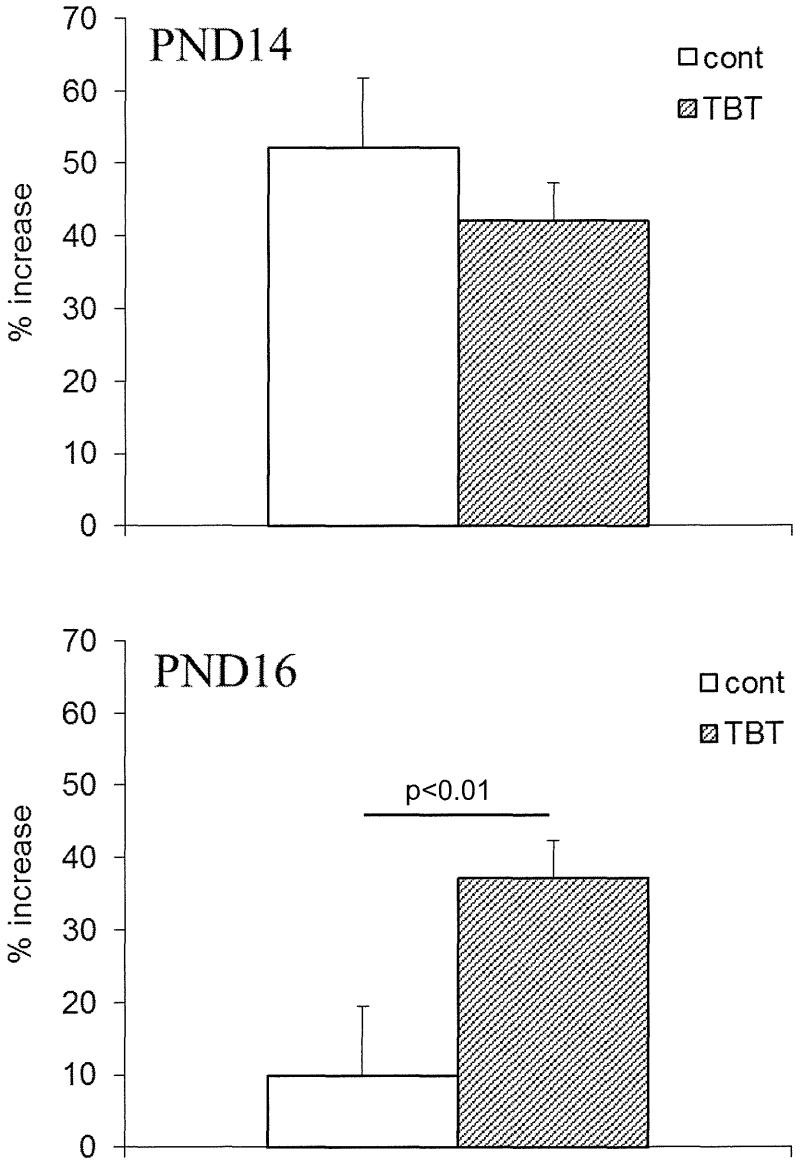

図 11. PND14 および PND16 における集合スパイク電位（PS）振幅（刺激電流値 600 μA）に対する $GABA_A$受容体拮抗薬ビククリン（BMI）の増強作用とこれに対する TBT 胎生期曝露の影響。変化率（%increase）は次式で求められている。
%increase＝(BMI 存在下の応答/非存在下の応答 - 1)×100

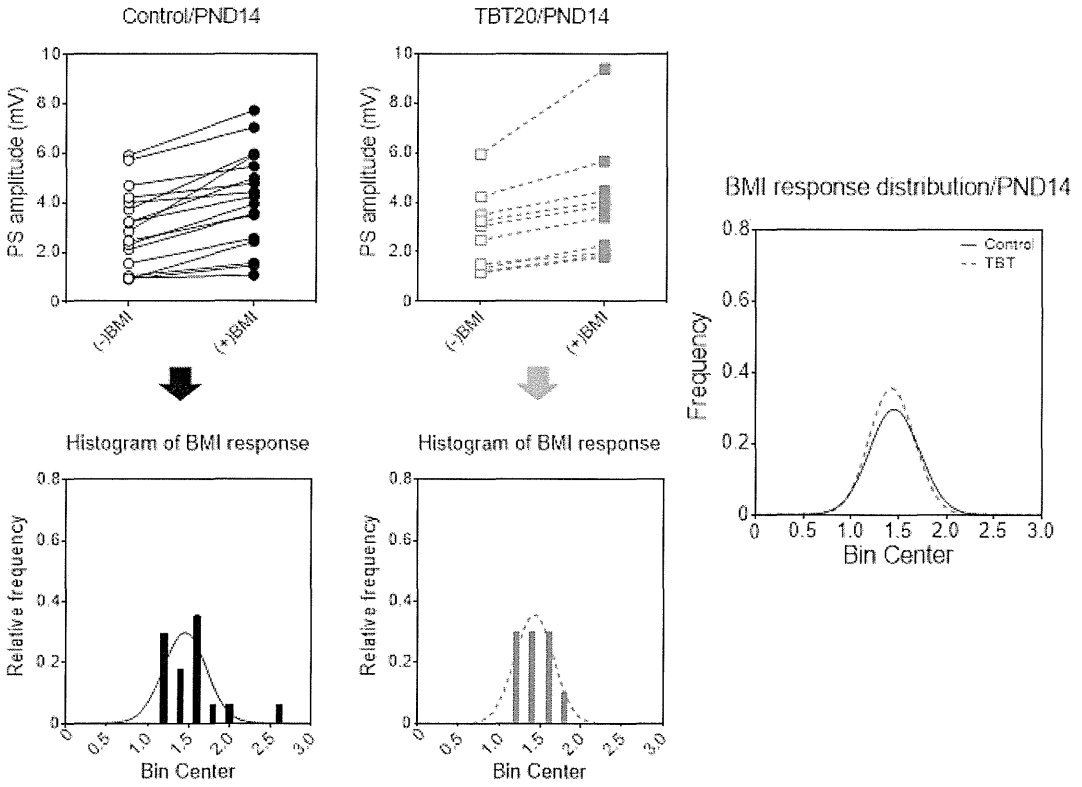

図 12. 生後 14 日齢における対照群と TBT20 群から得られた $GABA_A$受容体拮抗薬ビククリン（BMI）存在下、非存在下での集合スパイク電位（PS）振幅（刺激電流値 600 μ A）、および BMI による増強率の分布近似曲線。

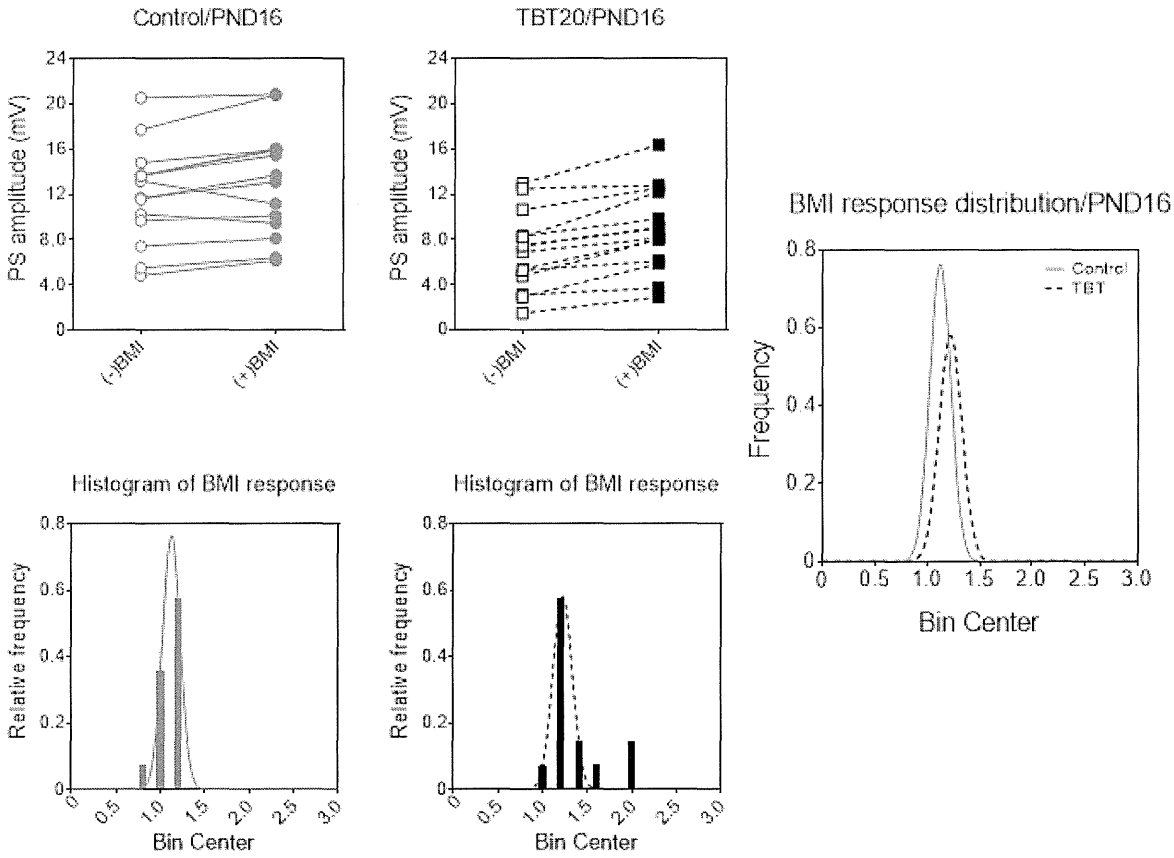

図 13. 生後 16 日齢における対照群と TBT20 群から得られた $GABA_A$受容体拮抗薬ビククリン（BMI）存在下、非存在下での集合スパイク電位（PS）振幅（刺激電流値 600 μA）、および BMI による増強率の分布近似曲線。

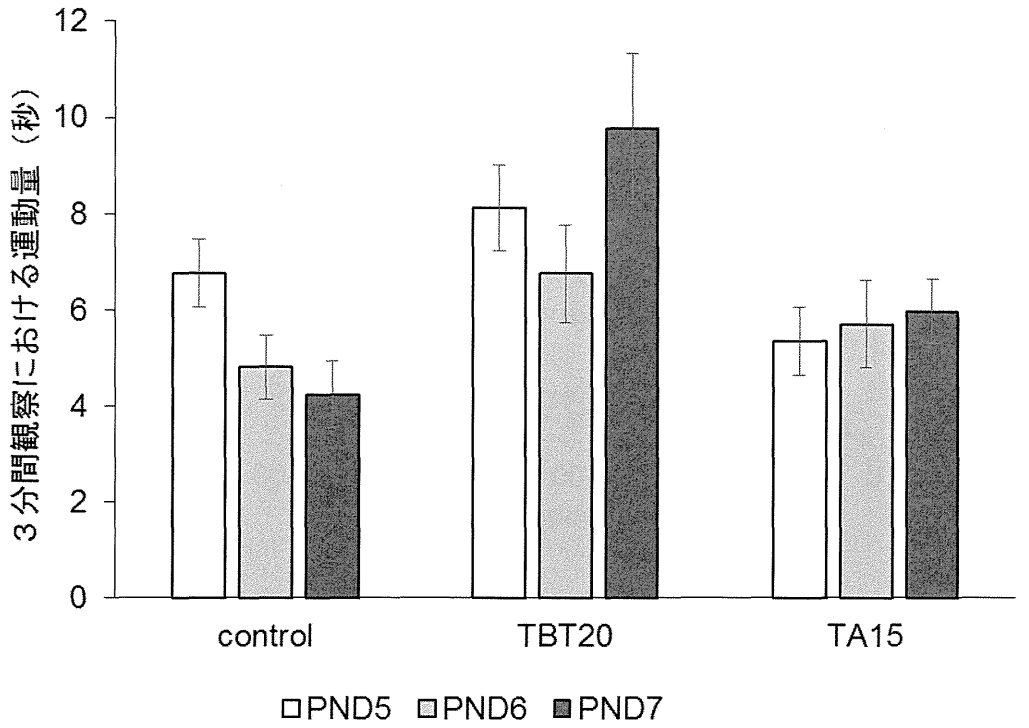

図 14. TBT、TA を胎生期に曝露された仔ラットの PND 5 から PND 7 までの間の不随意運動量の変化。不随意運動は３分間における運動量を秒数で示した（mean±SEM）。

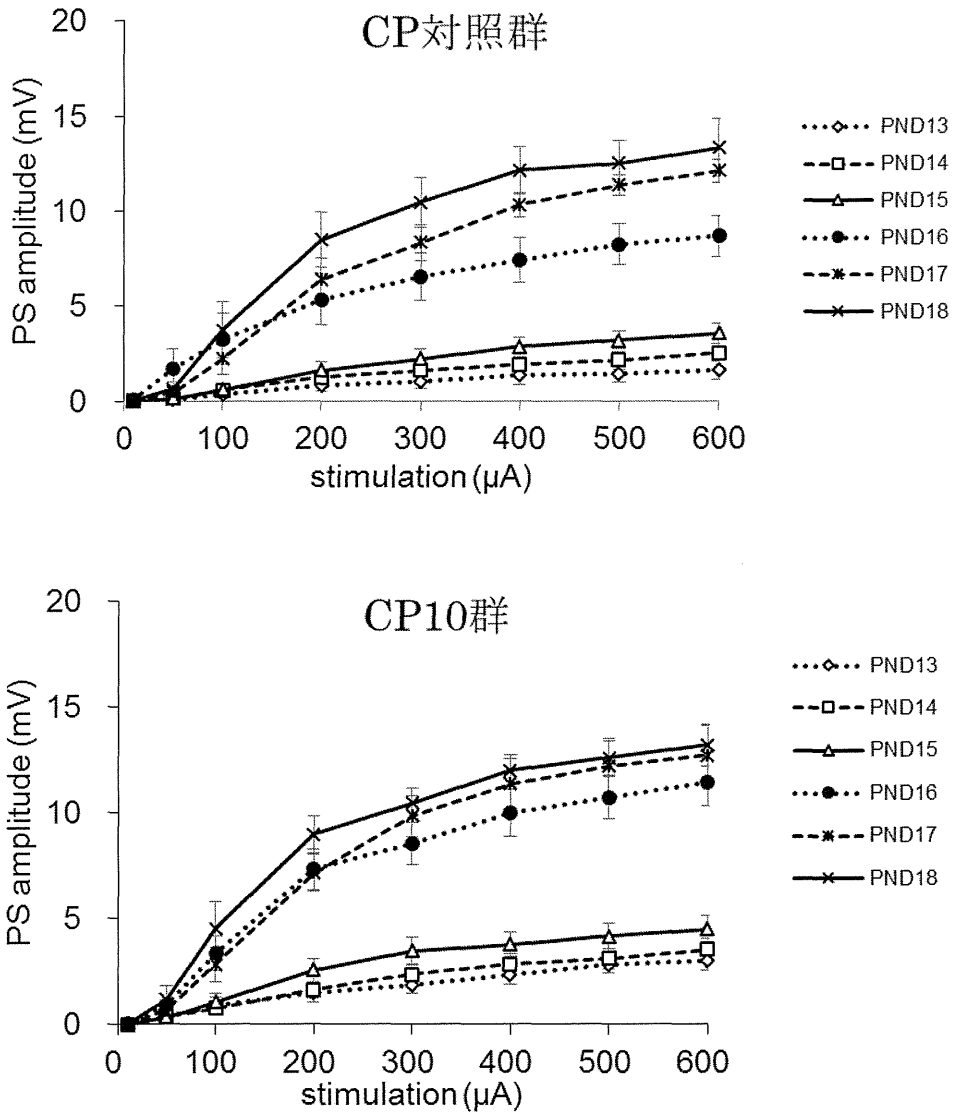

図 15. CP（10 mg/kg）を胎生期に曝露された仔ラットを用いて、生後日齢毎に得られた集合スパイク電位（PS）の刺激応答性。

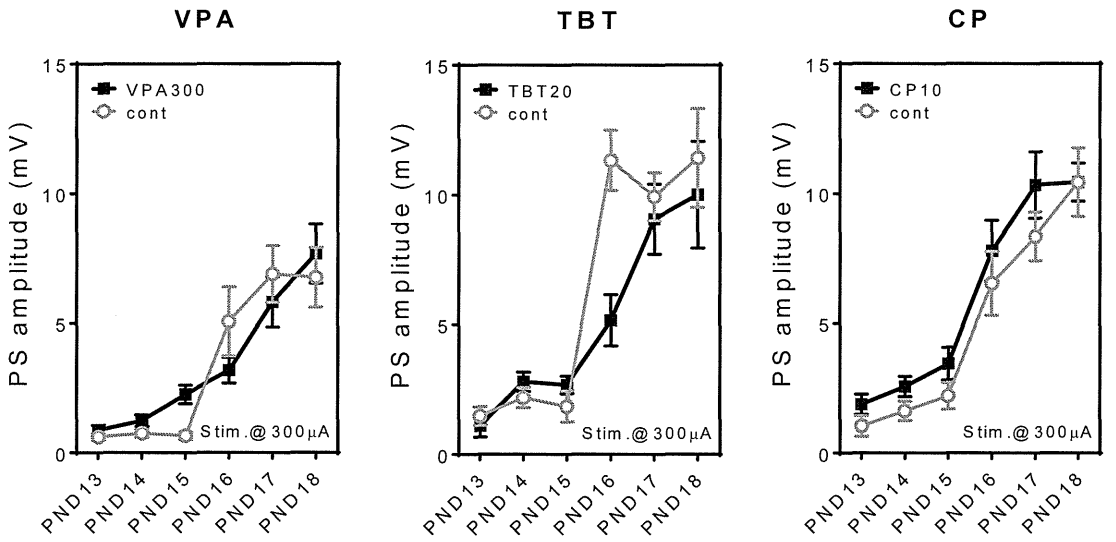

図 16. VPA、TBT、および CP を胎生期に投与された仔ラットから得られた集合スパイク電位（PS）の振幅と生後発達との関連性。
刺激電流値 300 μA で誘発された PS を各対照群と比較した。

III.　研究成果の刊行に関する一覧表

研究成果の刊行に関する一覧表

雑誌

発表者氏名	論文タイトル名	発表誌名	巻号	ページ	出版年
Ishida K., Kotake Y., Miyara M., Aoki K., Sanoh S., Kanda Y., Ohta S.	Involvement of GluR2 decrease in lead-induced neuronal cell death.	J. Toxicol. Sci.	38	513-521	2013
Yamada S., Kotake Y., Sekino Y., Kanda Y.	AMP-activated protein kinase-mediated glucose transport as a novel target of tributyltin in human embryonic carcinoma cells	Metallomics	5	484-491	2013
関野祐子、佐藤薫、諫田泰成、石田誠一	ヒトiPS分化細胞を利用した医薬品のヒト特異的有害反応評価系の開発・標準化	国立医薬品食品衛生研究所報告	131	25-34	2013
諫田泰成	ヒトiPS細胞から心筋細胞への分化誘導法	日本薬理学雑誌	141	32-36	2013
Yamada S., Kotake Y., Demizu Y., Kurihara M.,Sekino Y., Kanda Y.	Isocitrate dehydrogenase 3 as a novel target of tributyltin in human embryonic carcinoma cells.	Sci. Rep.	4	5952	2014
Nagakubo T., Demizu Y., Kanda Y., Misawa T., Shoda T., Okuhira K., Sekino Y., Naito M., Kurihara M.	Development of cell-penetrating R7 fragment-conjugated helical peptides as inhibitors of estrogen receptor-mediated transcription.	Bioconjugate Chem.	25	1921-1924	2014
Hirata N., Yamada S., Shoda T., Kurihara M., Sekino Y., Kanda Y.	Sphingosine-1-phosphate promotes expansion of cancer stem cells via S1PR3 by a ligand-independent Notch activation	Nature Commun.	5	4806	2014
Hayakawa T., Kunihiro T., Ando T., Kobayashi S., Matsui E., Yada H., Kanda Y., Kurokawa J., Furukawa T.	Image-based evaluation of contraction-relaxation kinetics of human-induced pluripotent stem cell-derived cardiomyocytes: correlation and complementarity with extracellular electrophysiology.	J. Mol. Cell. Cardiol.	77	178-191	2014
Hiyoshi H., Goto N., Tsuchiya M., Iida K., Nakajima Y., Hirata N., Kanda Y., Nagasawa K., Yanagisawa J.	YL-109 is a novel antitumor agent suppressing triple-negative breast cancer progression by inducing ubiquitin ligase CHIP.	Sci. Rep.	4	7095	2014
Tsuchiya M, Nakajima Y, Hirata N, Morishita T, Kishimoto H, Kanda Y, Kimura K.	Ubiquitin ligase CHIP suppresses cancer stem cell properties in a population of breast cancer cells.	Biochem Biophys Res Commun.	452	928-932	2014
Nakamura Y., Matsuo J., Miyamoto N., Ojima A., Ando K., Kanda Y., Sawada K., Sugiyama A., Sekino Y.	Assessment of testing methods for drug-induced repolarization delay and arrhythmias in an iPS cell-derived cardiomyocyte sheet: multi-site validation study.	J Pharmacol Sci.	124	494-501	2014
諫田泰成	ヒトiPS細胞を用いた成熟心筋細胞の開発	心電図	34	306-309	2014

澤田光平、松尾純子、長田智治、吉田善紀、白尾智明、佐藤薫、諫田泰成、関野祐子	霧島会議Stem Cell Safety Pharmacology Working Groupまとめ－ヒトES/iPS細胞由来心筋細胞を用いた催不整脈作用検出とその課題－	心電図	34	302-305	2014
諫田泰成	癌幹細胞の受容体を標的とした創薬の可能性	日本薬理学雑誌	144	17-21	2014
Yosuke D, Takashi Mi, Takaya N, Yasunari K, Keiichiro O, Yuko S, Mikihiko N, Masaaki K.	Structural development of stabilized helical peptides as inhibitors of estrogen receptor (ER)-mediated transcription.	Bioorg.Med.Chem.	23	4132-8	2015
Asakura K, Hayashi S, Ojima A, Taniguchi T, Miyamoto N, Nakamori C, Nagasawa C, Kitamura T, Osada T, Honnda Y, Kasai C, Ando H, Kanda Y, Sekino Y, Sawada K.	Improvement of acquisition and analysis methods in multi-electrode array experiments with iPS cell-derived cardiomyocyte.	Journal of Pharmacological and Toxicological Methods			2015
Yamada S., Kotake Y., Nakano M., Sekino Y. Kanda Y.	Tributyltin induces mitochondrial fission through NAD-IDH dependent mitofusin degradation in human embryonic carcinoma cells.	Metallomics	7	1240-6	2015
Asanagi M., Yamada S., Hirata N, Itagaki H., Kotake Y., Sekino Y. Kanda Y.	Tributyltin induces G2/M cell cycle arrest via NAD+-dependent isocitrate dehydrogenase in human embryonic carcinoma cells.	JTS	41	207-215	2016
Hirata N., Yamada S., Asanagi M., Sekino Y., Kanda Y.	Nicotine induces mitochondrial fission through mitofusin degradation in human multipotent embryonic carcinoma cells.	BBRC	470	300-5	2016
Kim S.-R., Kubo T., Kuroda Y., Hojyo M., Matsuo T., Miyajima A., Usami M., Sekino Y., Matsushita T., Ishida S.	Comparative metabolome analysis of cultured fetal and adult hepatocytes in humans.	J Toxicol Sci.	39	717-723	2014
Usami M., Mitsunaga K., Irie T., Miyajima A., Doi O.	Simple in vitro migration assay for neural crest cells and the opposite effects of all-trans-retinoic acid on cephalic- and trunk-derived cells.	Congenit Anom	54	184-188	2014
Usami M., Mitsunaga K., Irie T. Nakajima M.	Various definitions of reproductive indices: a proposal for combined use of brief definitions.	Congenital Anomalies	54	67-68	2014

Usami M., Mitsunaga K., Irie T., Miyajima A. Doi O.	Proteomic analysis of ethanol-induced embryotoxicity in cultured post-implantation rat embryos.	The Journal of Toxicological Sciences	39	285-292	2014
Usami M., Mitsunaga K., Miyajima A., Takamatu M., Kazama S., Irie T., Doi O., Takizawa T.	Effects of 13 developmentally toxic chemicals on the migration of rat cephalic neural crest cels in vitro.	Congenital Anomalies			2015
Irie T., Kikura-Hanajiri R., Usami M., Uchiyama N., Goda Y., Sekino Y	MAM-2201, a synthetic cannabinoid drug of abuse, suppresses the synaptic input to cerebellar Purkinje cells via activation of presynaptic CB1 receptors.	Neuropharmacology	95	479–91	2015
Oguchi-Katayama A., Monma A., Sekino Y., Moriguchi T., Sato K	Comparative gene expression analysis of the amygdalae of juvenile rats exposed to valproic acid at prenatal and postnatal stages.	J Toxicol Sci	38 (3)	381-402	2013
Takahashi K., Ishii-Nozawa R., Takeuchi K., Nakazawa K., Sekino Y., Sato K.	Niflumic acid activates additional currents of the human glial L-glutamate transporter EAAT1 in a substrate-dependent manner.	Biol Pharm Bull	36 (12)	1996-2004	2013
Fujimori, K., Takaki, J., Miura, M., Shigemoto-Mogami, Y., Sekino, Y., Suzuki, T., Sato, K.	Paroxetine prevented the down-regulation of astrocytic L-Glu transporters in neuroinflammation.	J Pharamcol Sci (in press)			
Shigemoto-Mogami, Y., Hoshikawa, K., Goldman, J.E.,Sekino, Y., Sato, K.	Microglia enhances neurogenesis and oligodendrogenesis in the early postnatal subventricular zone.	J Neurosci.	34(5)	2231-2243	2014
Shigemoto-Mogami, Y., Fujimori, K., Ikarashi, Y., Hirose, A., Sekino, Y., Sato, K.	Residual metals in carbon nanotubes suppress the proliferation of neural stem cells.	Fundam Toxcol Sci.	1(3)	87-94	2014
佐藤　薫	ミクログリアの発生と分化	Clinical Neuroscience	32 (12)	1338-1341	2015
Sato, K.	Microglia effects on neuronal development.	GLIA	63 (8)	1394-495	2015
吉田祥子・穂積直裕	神経伝達物質を視るデバイスが拓く神経科学の展開 ～ 求められる技術を開発する技術 ～	信学技報	112-345	39-40	2012
吉田祥子・穂積直裕	発達期小脳アストロサイトの機能と秩序形成	JNNS.	20	14-18	2013

K. Watanabe, N. Takahashi, N. Hozumi, S. Yoshida,	Improvements in Enzyme-Linked Photo assay Systems for Spatiotemporal Observation of Neurotransmitter Release	Sensors and Materials	27 (10)	1035–1044	2015
H. Mabuchi, HY Ong, K. Watanabe, S. Yoshida, N. Hozumi,	Visualization of Spatially Distributed Bioactive Molecules Using Enzyme-Linked Photo Assay	IEEJ Transactions (in press)			
上野　晋	化学物質（金属・有機溶剤）の毒性学と産業医としての対応	産業医科大学雑誌	第35巻特集号	91-6	2013
Park EK, Wilson D, Choi HJ, Wilson CT, Ueno S.	Hazardous metal pollution in the republic of Fiji and the need to elicit human exposure.	Environ Health Toxicol.			2013
Obara G., Toyohira Y., Inagaki H., Takahashi K., Horishita T., Kawasaki T., Ueno S., Tsutsui M., Sata T., Yanagihara N.	Pentazocine inhibits norepinephrine transporter function by reducing its surface expression in bovine adrenal medullary cells.	*J Pharmacol Sci.*	121	138-47	2013
Uchida T., Furuno Y., Tanimoto A., Toyohira Y., Arakaki K., Kina-Tanada M., Kubota H., Sakanashi M., Matsuzaki T., Noguchi K. Nakasone J., Igarashi T., Ueno S., Matsushita M., Ishiuchi S., Masuzaki H., Ohya Y., Yanagihara N., Shimokawa H., Otsuji Y., Tamura M., Tsutsui M.	Development of an experimentally useful model of acute myocardial infarction: 2/3 nephrectomized triple nitric oxide synthases-deficient mouse.	J Mol Cell Cardiol.	77	29-41	2014
Horishita T., Yanagihara N., Ueno S., Sudo Y., Uezono Y., Okura D., Minami T., Kawasaki T., Sata T.	Neurosteroids allopregnanolone sulfate and pregnanolone sulfate have diverse effect on the a subunit of the neuronal voltage-gated sodium channels Nav1.2, Nav1.6, Nav1.7, and Nav1.8 expressed in *Xenopus* oocytes.	Anesthesiology.	121	620-631	2014
Okura D., Horishita T., Ueno S., Yanagihara N., Sudo Y., Uezono Y., Sata T.	The endocannabinoid anandamide inhibits voltage-gated sodium channels Nav1.2, Nav1.6, Nav1.7 and Nav1.8 in Xenopus oocytes.	Anesth. Analg.	118	554-62	2014
Yanagihara N, Zhang H, Toyohira Y, Takahashi K, Ueno S, Tsutsui M, Takahashi K.	New insights into the pharmacological potential of plant flavonoids in the catecholamine system.	J Pharmacol Sci.	124	123-8	2014

Inagaki H, Toyohira Y, Takahashi K, Ueno S, Obara G, Kawagoe T, Tsutsui M, Hachisuga T, Yanagihara N.	Effects of selective estrogen receptor modulators on plasma membrane estrogen receptors and catecholamine synthesis and secretion in cultured bovine adrenal medullary cells.	J Pharmacol Sci.	124	66-75	2014
Okura D., Horishita T., Ueno S., Yanagihara N., Sudo Y., Uezono Y., Minami T., Kawasaki T., Sata T.	Lidocaine preferentially inhibits the function of purinergic P2X7 receptors expressed in *Xenopus* Oocytes.	Anesth Analg.	120	597-605	2015
Ishidao T, Fueta Y, Ueno S, Yoshida Y, Hori H.	A cross-fostering analysis of bromine ion concentration in rats that that inhaled 1-bromopropane vapor.	*J. Occup. Health*, in press.			
Fueta Y, Kanemitsu M, Egawa S, Ishidao T, Ueno S, Hori H.	Prenatal exposure to 1-bromopropane suppresses kainate-induced wet dog shakes in immature rats.	*J UOEH.*	37	255-261	2015
Li X, Toyohira Y, Horisita T, Satoh N, Takahashi K, Zhang H, Iinuma M, Yoshinaga Y, Ueno S, Tsutsui M, Sata T, Yanagihara N.	Ikarisoside A inhibits acetylcholine-induced catecholamine secretion and synthesis by suppressing nicotinic acetylcholine receptor-ion channels in cultured bovine adrenal medullary cells.	*Naunyn Schmiedebergs Arch Pharmacol.*	388	1259-1269	2015

書籍

著者氏名	論文タイトル名	書籍全体の編集者名	書　籍　名	出版社名	出版地	出版年	ページ
Kanda Y.	Assessment of cigarette smoking toxicity using cancer stem cells.	Nazmi Sari	Smoking Restrictions, Risk Perceptions and Its Health and Environmental Impacts	Nova Science Publishers	United States of America	2014	185-196
Kanda Y.	1. Cancer Stem Cells - Fact or Fiction?	Dittmar T, Zänker KS	Role of Cancer Stem Cells in Cancer Biology and Therapy	CRC Press	United States of America	2013	1-22
諫田泰成	ヒトiPS細胞を用いた心毒性試験の現状と課題	安全性評価研究会編集委員会	谷本学校毒性質問箱第16号	株式会社サイエンティスト社	東京	2014	91-94
諫田泰成	再生心筋細胞を用いた安全性薬理評価系の開発	エイブル株式会社和田昌憲	再生医療における臨床研究と製品開発	技術情報協会	東京	2013	572-576

IV.　研究成果の刊行物・別刷

The Journal of Toxicological Sciences (J. Toxicol. Sci.)
Vol.38, No.3, 513-521, 2013

Original Article

Involvement of decreased glutamate receptor subunit GluR2 expression in lead-induced neuronal cell death

Keishi Ishida[1], Yaichiro Kotake[1], Masatsugu Miyara[1], Kaori Aoki[1], Seigo Sanoh[1], Yasunari Kanda[2] and Shigeru Ohta[1]

[1]Graduate School of Biomedical and Health Sciences, Hiroshima University, 1-2-3 Kasumi, Minami-ku, 734-8553, Japan
[2]Division of Pharmacology, National Institute of Health Sciences, 1-18-1, Kamiyoga, Setagaya-ku 158-8501, Japan

(Received April 4, 2013; Accepted April 25, 2013)

ABSTRACT — Lead is known to induce neurotoxicity, particularly in young children, and GluR2, an AMPA-type glutamate receptor subunit, plays an important role in neuronal cell survival. Therefore, we hypothesized that altered GluR2 expression plays a role in lead-induced neuronal cell death. To test this idea, we investigated the effect of exposure to 5 and 20 μM lead for 1-9 days on the viability and GluR2 expression of primary-cultured rat cortical neurons. The number of trypan-blue stained cells was increased by exposure to 5 μM lead for 9 days or 20 μM lead for 7-9 days, and LDH release was increased after exposure to 20 μM lead for 9 days. GluR2 expression was reduced by exposure to 5-100 μM lead, but not 0.1-1 μM lead, for 9 days. Immunocytochemistry also confirmed that GluR2 expression was decreased in the presence of lead. Application of 50 ng/ml brain-derived neurotrophic factor (BDNF) led to a recovery of lead-induced neuronal cell death, accompanied with increased GluR2 expression. Our results suggest that long-term exposure to lead induces neuronal cell death, in association with a decrease of GluR2 expression.

Key words: Lead, GluR2, Brain-derived neurotrophic factor

INTRODUCTION

Lead has been widely used in many products; for example, leaded gasoline, lead-based paint, and cans containing foods or alcoholic beverages. Exposure to high levels of environmental lead causes various public health problems, particularly among young children, because of its effects on the blood and brain, including disruption of nervous system communication (Gracia and Snodgrass, 2007). Recently, regulation of industrial and environmental levels of lead has been strengthened in many countries, but soil and water contamination is a persistent source of lead exposure in industrialized societies. Toxicity typically results from ingestion of food or water contaminated with lead, but may also occur after accidental ingestion of contaminated dust, soil, or lead-containing paints (Gracia and Snodgrass, 2007). Over 90% of lead absorbed after inhalation or oral ingestion is retained in the body and distributed to the bones (Links *et al.*, 2001), where the half-life of lead is decades long. It was reported that individuals with baseline blood lead levels of 10 to 19 μg/dl suffer increased mortality from various causes: for example, mortality due to circulatory disease was increased by 10% and mortality due to cancer was increased by 46% relative to individuals with blood lead levels of less than to 10 μg/dl (Lustberg and Silbergeld, 2002). Thus, blood lead level is positively associated with mortality due to circulatory disorders and cancers.

Lead is known to induce neurotoxicity, leading to lowered intelligence test scores, behavioral problems and decreased cognitive ability (Canfield *et al.*, 2004; Laidlaw *et al.*, 2005). Lead-related intellectual deficits are seen in children with blood lead levels of at least 10 μg/dl, though no evidence of a threshold was found (Lanphear *et al.*, 2005). Schoolchildren with elevated blood lead levels due to both pre- and postnatal lead exposure are more likely to exhibit disruptive behavior in class (Leviton *et al.*, 1993; Bellinger *et al.*, 1994). Moreover, childhood exposure to lead is a risk factor for attention-deficit/hyperactivity disorder (ADHD) (Froehlich *et al.*,

Correspondence: Yaichiro Kotake (E-mail: yaichiro@hiroshima-u.ac.jp)

2009). However, the mechanisms involved have not been clarified in detail.

Glutamate is an essential amino acid in the central nervous system. Glutamate receptors affect the survival and maturation of cortical, mesencephalic, and cerebellar granule neurons (Blandini *et al.*, 1996; Monti *et al.*, 2002; Hirasawa *et al.*, 2003), and play a central role in learning and memory. Ca^{2+} influx through glutamate receptors due to excitotoxic and ischemic damage can trigger multiple intracellular cascades and cause damage to neuronal cells in the brain (Choi, 1988; Tymianski, 1996; Ying *et al.*, 1997). Ionotropic glutamate receptors are mainly divided into two types, *N*-methyl-D-aspartate (NMDA) receptors and α-amino-3-hydroxy-5-methylisoxazole-4-propionic acid (AMPA) receptors. NMDA receptors are composed of an obligatory NR1 subunit and accessory subunits from the NR2 or NR3 family and the latter subunits are expressed differentially during development. Each subunit plays a specific role, contributing to the subcellular localization and channel properties of NMDA receptors (Luo *et al.*, 2011). Thus, changes of NMDA receptor subunit composition influence neuronal activity and survival. On the other hand, AMPA receptors are heteromeric complexes composed of four subunits (GluR1 to GluR4). Among the AMPA receptor subunits, GluR2 is expressed widely in hippocampal pyramidal and granule neurons (Hollmann and Heinemann, 1994) and in cortical neurons (Kondo *et al.*, 1997). AMPA receptor channel impermeability to Ca^{2+} is dependent upon the GluR2 subunit, and cells that contain AMPA receptor lacking the GluR2 subunit show high Ca^{2+} permeability and vulnerability to excitotoxicity (Liu and Zukin, 2007).

Lead is a potent, non-competitive and voltage-independent antagonist of NMDA receptor (Alkondon *et al.*, 1989). It is reported that lead binding at the Zn^{2+}-binding site of NMDA receptor is dependent on the receptor composition, i.e., lead showed competitive inhibition at the Zn^{2+} binding site of NR2A, but not at the Zn^{2+} binding site of NR2B (Gavazzo *et al.*, 2008). Moreover, lead alters NMDA receptor subunit composition. Expression of NR2A and NR1 is decreased (Nihei *et al.*, 2000) and the expression of NR1 splice variant mRNA is altered (Guilarte *et al.*, 2000) in rat hippocampus following exposure to lead. Further, lead exposure during synaptogenesis changes NMDA receptor expression at developing synapses (Neal *et al.*, 2011). Thus, lead-induced changes of NMDA receptor subunit composition may result in disruption of downstream signaling. However, the effects of lead on AMPA receptors have not been investigated. Therefore, in the present work, we investigated the effect of lead on the viability and GluR2 expression of primary-cultured rat cortical neurons to test our hypothesis that decreased GluR2 expression is involved in lead-induced neuronal cell death.

MATERIALS AND METHODS

Materials

Eagle's minimal essential salt medium (Eagle's MEM) was purchased from Nissui Pharmaceutical (Tokyo, Japan). Fetal calf serum (FCS) was purchased from Nichirei Biosciences Inc. (Tokyo, Japan). Horse serum (HS) was purchased from Gibco (Life Technologies, Carlsbad, CA, USA). Trypan blue, D-(+)-glucose, $NaHCO_3$, sodium orthovanadate, phenylmethylsulfonyl fluoride (PMSF), sodium dodecyl sulfate (SDS), glycerol, and paraformaldehyde were purchased from Wako (Tokyo, Japan). Lead acetate was purchased from EBISU (Osaka, Japan). HEPES was purchased from DOJINDO (Kumamoto, Japan). L-Glutamine, arabinocylcytosine, formaldehyde and anti-β-actin antibody (AC-15) were purchased from Sigma-Aldrich (St. Louis, MO, USA). Pentobarbital was purchased from Kyoritsu (Tokyo, Japan). Bromophenol blue was purchased from Katayama Chemical Industries Co., Ltd. (Osaka, Japan). Tris-HCl, nonidet P-40, EDTA, mercaptoethanol and Protease Inhibitor Cocktail was purchased from Nacalai Tesque (Kyoto, Japan). Anti-GluR2 antibody (MAB397) was purchased from Millipore (Billerica, MA, USA). Anti-N-cadherin antibody (sc-7939) was purchased from Santa Cruz Biotechnology (Dallas, TX, USA).

Cell culture

The following procedures were performed under sterile conditions. The present study was approved by the university's animal ethics committee of Hiroshima University. Primary cultures were obtained from cerebral cortex of fetal rats at 18 days of gestation. Fetuses were taken from pregnant Slc:Wistar/ST rats under pentobarbital anesthesia. The prefrontal part of the cerebral cortex was dissected with a razor blade, and cells were dissociated by gentle pipetting. Dissociated cells were plated on culture plates (4×10^5 cells/cm^2). Cultures were incubated in Eagle's MEM supplemented with 10% heat-inactivated FCS, L-glutamine (2 mM), D-(+)-glucose (11 mM), $NaHCO_3$ (24 mM), and HEPES (10 mM). Cultures were maintained at 37°C in an atmosphere of humidified 5% CO_2 in air. The cultures were incubated in MEM containing 10% FCS (days *in vitro* (DIV) 1-7) or 10% HS (DIV 8-11). The medium was exchanged every 2 days. Arabinocylcytosine (10 μM) was added to inhibit the proliferation of non-neuronal cells after DIV 6. Cultures were

used for experiments at DIV 11. This protocol has been confirmed to produce cultures containing about 90% neurons by immunostaining for a neuron marker MAP2.

Treatment of cultures

Medium containing lead was changed at DIV 2, 4, 6, 8, and 10 and the neurons were exposed until DIV 11 for 9 days. In BDNF experiment, BDNF was added to the culture medium at DIV 2 and further added every day until DIV 10. Thus, the neurons were exposed also with BDNF for 9 days.

Trypan blue assay

After exposure to lead acetate, cell cultures were stained with 1.5% trypan blue for 10 min, then fixed with 10% formalin for 2 min, and rinsed with physiological saline. Unstained cells were regarded as viable and stained cells were regarded as dead. The viability of the cultures was calculated as the percentage ratio of the number of unstained cells to the total cells counted. Over 200 cells per cover slip were randomly counted.

LDH assay

LDH release was measured using a CytoTox 96 Non-Radioactive Cytotoxicity Assay (Promega®) according to the manufacturer's protocol. After exposure to lead acetate, culture medium (50 μl) was transferred to a 96-well plate. Substrate mixture (50 μl) was added to each well and allowed to react for 30 min in the dark at room temperature. Stop solution (50 μl) was then added to each well, and the absorbance was read at 490 nm. The absorbance was normalized based on the absorbance of negative controls, which consisted of cells not exposed to lead.

Western blotting

After lead acetate treatment, cells were washed with PBS buffer and lysed in TNE buffer containing 50 mM Tris-HCl, 1% nonidet P-40, 20 mM EDTA, Protease Inhibitor Cocktail (1:200), 1 mM sodium orthovanadate, and 1 mM PMSF. The mixture was rotated at 4°C and centrifuged at 15,000 rpm, after which the supernatant was transferred to a microtube. The supernatant was added to sample buffer containing 100 mM Tris-HCl, 4% SDS, 20% glycerol, 0.004% bromophenol blue, and 5% mercaptoethanol, and then denatured at 95°C for 3 min. Protein was separated by SDS-polyacrylamide gel electrophoresis and transferred to a polyvinylidene difluoride membrane. The membrane was blocked with blocking buffer containing 5% skim milk for 1 hr, and then incubated with anti-GluR2 (1:2,000) and anti-β-actin (1:4,000) overnight, and with secondary antibody for 1 hr. Other details were performed by the methods described previously (Hashida *et al.*, 2011). The protein was detected with an enhanced chemiluminescence detection system (Chemi-Lumi One L, Nacalai Tesque (Kyoto, Japan)). Quantitative analysis was performed with digital imaging software (Image J, NIH (Bethesda, MD, USA)), and GluR2 protein levels were corrected on the basis of β-actin protein levels.

Immunocytochemistry

Cells were seeded in poly-D-lysine-coated 8-well chamber slides (BD BioCoat™) and incubated overnight. After treatment with 5 and 20 μM lead for 9 days, cells were washed with PBS(-) and fixed with 4% paraformaldehyde in PBS(-) for 15 min at room temperature. The slides were washed with PBS(-), blocked with 4 drops of Image-iT™ FX Signal Enhancer (Molecular Probes®) for 1 hr, and incubated with mouse anti-GluR2 (MAB397), which recognizes the N-terminal extracellular domain of GluR2 (1:250), and rabbit anti-N-cadherin (1:250) diluted in PBS(-) overnight at 4°C. Then, the slides were washed three times with PBS(-), and incubated with Alexa Fluor® 488-conjugated goat anti-mouse IgG (1:800, Molecular Probes®) and Alexa Fluor® 555-conjugated goat anti-rabbit IgG (1:800, Molecular Probes®) for 1 hr at room temperature in the dark. The slides were further washed three times with PBS(-), incubated with 4',6-diamidino-2-phenylindole dihydrochloride (DAPI, 1:2,000, Molecular Probes®) diluted in PBS(-) for 5 min, and washed again three times with PBS(-). Finally, the slides were enclosed in Prolong® Gold (Molecular Probes®) and observed under a confocal laser scanning microscope (Olympus, FV-1000-D).

Statistics

All the experiments were performed at least three times and representative data are shown. Data are expressed as mean + S.E.M. Statistical evaluation of the data was performed with ANOVA followed by Tukey's test. A value of $P < 0.05$ was considered to be indicative of significance.

RESULTS

Lead-induced cell death of cortical neurons

First, we investigated neuronal cell death induced by long-term exposure to lead. Rat cortical neurons were exposed to 5 and 20 μM lead for 1, 3, 5, 7, and 9 days, and then the cell viability was examined by means of trypan blue assay (Fig. 1A) and LDH assay (Fig. 1B). Exposure of the cells to 5 μM lead for 9 days resulted in a decrease of the cell viability to 29% of the control, while